Rotationinduced vibrational mixing in S 1 H2CO near E′vib =2000–2300 cm− 1: 2143 and 214161 levels

Eric C. Apel and Edward K. C. Lee

Citation: The Journal of Chemical Physics **85**, 1261 (1986); doi: 10.1063/1.451264
View online: http://dx.doi.org/10.1063/1.451264
View Table of Contents: http://scitation.aip.org/content/aip/journal/jcp/85/3?ver=pdfcov
Published by the AIP Publishing

Rotation-induced vibrational mixing in S_1 H_2CO near $E'_{vib} = 2000$–2300 cm^{-1}: $2^1 4^3$ and $2^1 4^1 6^1$ levels[a)]

Eric C. Apel[b)] and Edward K. C. Lee
Department of Chemistry, University of California, Irvine, California 92717

(Received 10 March 1986; accepted 7 April 1986)

Coriolis-induced vibrational mixing in S_1 H_2CO near $E'_{vib} = 2000$–2300 cm^{-1} is manifested by the rotational quantum number (J', K'_a) dependent variation of the emission intensity in the rotationally resolved, dispersed fluorescence spectrum. The **c**-axis Coriolis resonance between $2^1 4^3$ ($K'_a = 5$) and $2^1 4^1 6^1$ ($K'_a = 4$) is observed with $\xi^{(c)}_{st} \simeq 0.2$ cm^{-1}. The **b**-axis Coriolis interaction between $2^1 4^1 6^1$ ($K'_a = 5$) and $4^4 6^1$ ($K'_a = 4$) in S_1 as well as the **a**-axis Coriolis interaction between 4_2 and $4_1 6_1$ in S_0 are observed. A significant degree of vibrational mixing is observed in the energy range, $E'_{vib} = 2000$–2300 cm^{-1}.

I. INTRODUCTION

Intramolecular vibrational redistribution (IVR) has received much recent attention both theoretically[1–5] and experimentally.[6–12] It plays an important role in the relaxation dynamics of excited polyatomic molecules, because it can favorably compete with electronic relaxation processes as well as with collisional processes even at relatively low vibrational excitation energies (< 1000 cm^{-1}) and at high pressures, particularly for large polyatomics. Therefore, a variety of theoretical and experimental approaches to characterize and study the dynamics of IVR have been undertaken to observe IVR directly, and some excellent examples are in the literature as mentioned above. To what extent the two close-lying levels have mixed-in "relevant" vibrational components (in a zero-order basis set) and how the coupling can significantly affect intramolecular as well as intermolecular relaxation dynamics between them are little known. An interesting example of the effect of Coriolis-enhanced rotational selectivity on mode-to-mode vibrational energy transfer in S_0 D_2CO has been reported only recently.[13] Small or medium-size molecules are ideal for obtaining detailed spectroscopic information on rotation-induced vibrational state mixing, and therefore a few recent studies have focused on this important problem in such molecules as H_2O,[14(a),15] H_2CO[9,14(b),16–18] and C_6H_6.[10] In this paper, we wish to report rotation-induced vibrational mixing in the $E'_{vib} = 2000$–2300 cm^{-1} region of S_1 H_2CO. This work is complementary to an earlier investigation[16] in our laboratory that dealt with the $E'_{vib} \simeq 3000$ cm^{-1} region involving 5^1 and $1^1 4^1$ levels of S_1 H_2CO.

A set of nine vibrational levels of interest here (within ~ 150 cm^{-1} of $2^1 4^3$) is shown in Fig. 1 and these are grouped into four vibrational symmetry species of the C_{2v} point group. Each vibrational symmetry species may be Coriolis coupled to three other vibrational symmetry species through molecular rotations about three principal axes as shown schematically at the bottom of Fig. 1. The selection rules and matrix elements for the rotation–vibration perturbations for C_{2v} molecules[19] are summarized in Table I. Sethuraman *et al.*[20] were the first to study the extensive pattern of perturbations in the $2^1_0 4^3_0$ absorption band in this energy region,[20] and Kerr *et al.*[21] have more recently analyzed the magnetic rotation spectra of this band with respect to singlet–triplet perturbations as well as singlet–singlet perturbations. In our work, we used a laser induced fluorescence probe and studied the rotationally resolved, dispersed fluorescence emission spectra from rotational levels of two vibrational states, $2^1 4^1 6^1$ and $2^1 4^3$, which are mixed with other nearby *zero-order* vibrational levels by Coriolis interactions. Preliminary results from this work have been reported,[17] and we shall use the previously used notation in which a *zero-order* vibrational state will be designated by bold faced letters (or an underline). The two-state-mixed eigenstates will be represented by two zero-order rovibrational wave functions, $|v_1,J,K\rangle$ and $|v_2,J,K\,(\text{or}\,K \pm 1)\rangle$, the mixing coefficients, d and g, and $\sigma_{\zeta k} = (\text{sign}\,\zeta)(\text{sign}\,k)$,

$$|\Psi_+\rangle = d\,|v_1,J,K\rangle - i\sigma_{\zeta k} g |v_2,J,K(\text{or}\ K \pm 1)\rangle \quad (1)$$

and

$$|\Psi_-\rangle = -i\sigma_{\zeta k} g |v_1,J,K\rangle + d\,|v_2,J,K(\text{or}\ K \pm 1)\rangle, \quad (2)$$

as previously applied[16,18] to nearly symmetric top molecules.

II. EXPERIMENTAL

The rotational levels of S_1 H_2CO were prepared by the laser excitation of S_0 H_2CO rotational levels populated at room temperature. A Nd:YAG pumped dye laser (Quanta-Ray DCR-1/PDL-1) equipped with an intracavity etalon (pressure tuned) was used as the excitation source. The dye laser was operated at a repetition rate of 10 Hz using laser dye (Exciton DCM in methanol) which has a tuning range of 620–680 nm. A pulse width of ~ 7 ns was obtained. The visible output of the dye laser was frequency doubled with an extracavity SHG crystal which gave a UV output pulse energy of 1–3 mJ and a bandwidth of $\leqslant 0.08$ cm^{-1} (FWHM). Since both S_1 and S_0 H_2CO are only slightly asymmetric, near prolate rotors, the asymmetry doublet splitting for rotational levels with moderate rotational energies ($J = 4$–14, $K_a = 4$–7) that were chosen for the present study is less than the Doppler width (~ 0.06 cm^{-1} near 330 nm at room tem-

[a)] The research has been supported by the National Science Foundation Grants CHE-82-17121/CHE-85-18874 and a grant from the Petroleum Research Fund administered by the American Chemical Society, No. 15092-AC6.

[b)] Present Address: Los Alamos National Laboratory, University of California, Los Alamos, NM 87544.

 0021-9606/86/151261-15$02.10

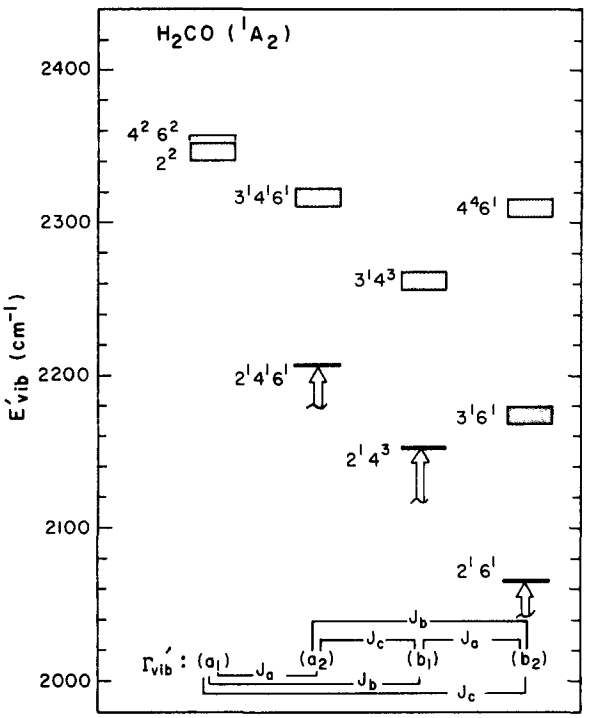

FIG. 1. Energy level diagram for nine vibrational eigenstates of H_2CO ($\tilde{A}\,^1A_2$) with excess vibrational energy (E'_{vib}) between 2000 and 2400 cm^{-1}. The vibrational levels are grouped according to the C_{2v} point group symmetry species, Γ'_{vib}. The rotational operator (J_g) connects each pair of vibrational species according to the rules summarized in Table I. For the planar ground electronic state of H_2CO ($\tilde{X}\,^1A_1$), the **a** axis lies along the C=O bond, the **b** axis lies in the molecular plane but perpendicular to the C=O bond, and the **c** axis is perpendicular to both the molecular plane and the C=O bond. The uncertainty in the vibrational origin is indicated by the hatched block.

perature). Thus we were unable to excite selectively one of the asymmetry doublet pair, i.e., a single rotational level (SRL). However, for all practical purposes considered in this work, this is not a significant limitation and we can approximate the prepared system as an SRL of a prolate top with the quantum numbers J and K. Nonetheless, the optical and the Coriolis interaction selection rules for the asymmetric rotor with J, M, K_a, and K_c quantum numbers are more appropriate for this system.

Monomeric H_2CO in the gas phase was produced by heating the solid H_2CO polymer at ~ 100 °C in a vacuum line. Gaseous H_2CO was condensed and kept under vacuum at liquid nitrogen temperature, until it was used to fill a static fluorescence cell to a pressure of 200–400 mTorr at room temperature. The complete description of the 35 ℓ cell with multipath optics, a 1 m scanning monochromator and associated gated electronics for fluorescence pulse detection is given elsewhere.[22] Fluorescence emission (FEM) spectra were recorded by scanning the wavelength of the monochromator, while the laser wavelength remained tuned to the line center of a rovibronic transition of interest. Fluorescence excitation spectra were recorded by scanning the wavelength of the laser during the collection of either a *broad* bandpass of the emission (e.g., 340–440 nm using a set of glass filters) or a *narrow* bandpass of the specific rovibronic emission (e.g., 348.5–349.3 nm). We shall call the former the fluorescence excitation spectrum for "total" emission (abbreviated as FEX) and latter the "rovibronic emission locked" fluorescence excitation spectrum (abbreviated as RELFEX). The rotational profile of the S_1–S_0 absorption of H_2CO was recorded by either an FEX or an RELFEX spectrum. Often, the laser frequency was calibrated by simultaneously recording the I_2 absorption spectrum[23] to a probable accuracy of ~ 0.02 cm^{-1}. The monochromator wavelengths were calibrated with a neon lamp to a probable accuracy of ~ 0.5 Å (~ 4 cm^{-1} in the 3500 Å region). A typical monochromator bandpass used in the UV region was 1.0 Å (8 cm^{-1} at 3500 Å in the second order of the diffraction grating using 0.200 mm slit widths) for recording an FEM spectrum and 8 Å (~ 65 cm^{-1} at 3500 Å) for recording an RELFEX spectrum. A 2 in. diameter, front face, blue sensitive photomultiplier (RCA 8575, 35 CT spectral response or EMI 9863 QB) was used as the detector of fluorescence. A typical setting for the gatewidth of the boxcar integrator (EG&G PAR 162/165) was 50 ns, which was optimum for detecting the fluorescence signal which decayed with $\tau = 15$–60 ns.

III. RESULTS

A. Fluorescence excitation spectra

Fluorescence excitation spectra were recorded over most of the rotational subbands of the $2_0^1 4_0^3$ vibronic band. The FEX spectrum recorded in the 30 418–30 390 cm^{-1} region is shown in panel (b) of Fig. 2. For comparison, an FTUV absorption spectrum recorded in the same region at approximately Doppler resolution of FWHM = 0.06 cm^{-1} (courtesy of D. A. Ramsay and W. S. Neil, National Research Council, Ottawa, Canada) is shown in panel (a) of Fig. 2. Since some of the rovibronic transitions in H_2CO (S_1–S_0) can come close to being saturated and being power broadened under the present experimental conditions, cau-

TABLE I. Summary of the possible rovibrational perturbations for C_{2v} molecules [taken from Clouthier and Ramsay (Ref. 19)].

$\Gamma_1^v \times \Gamma_2^v$	Type	Matrix element	ΔK_a	ΔK_c
A_1	Fermi	W_{12}	0	0
A_2	*a*-type Coriolis	$\xi_{12}^a K_a$	0	± 1
B_1	*b*-type Coriolis	$\xi_{12}^b [J(J+1) - K_a(K_a \pm 1)]^{1/2}$ [a]	± 1	∓ 1
B_2	*c*-type Coriolis	$\xi_{12}^c [J(J+1) - K_a(K_a \pm 1)]^{1/2}$ [a]	± 1	$0, \mp 2$

[a] The sign ($\pm$) is taken according to $\Delta K_a = \pm 1$; higher order perturbations are not considered [see Ref. 9(a)].

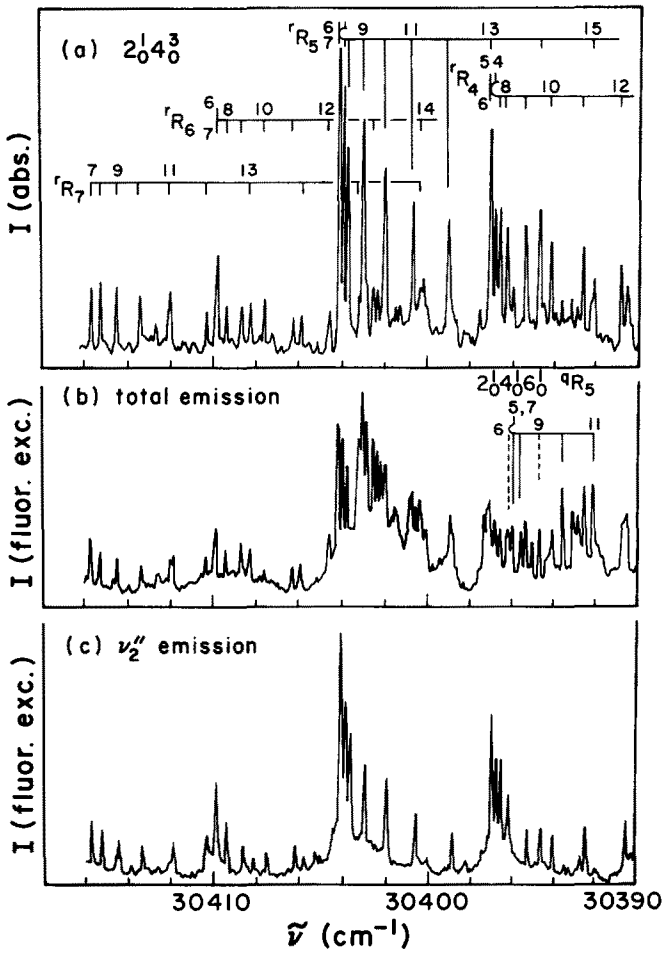

FIG. 2. A comparison of an FT absorption spectrum in the ^rR subband region ($K_a' = 4$–7) of the $2_0^1 4_0^3$ transition (a, upper panel, courtesy of Ramsay and Neil), an FEX spectrum of the "total" emission through a 340–440 nm bandpass (b, middle panel), and an RELFEX spectrum of the emission "locked onto" the ^rR transition terminating on the ν_2'' level at 3489 Å with an 8 Å bandpass, (c, lower panel)—a fingerprint of the $2_0^1 4_0^3$ transition. The rovibronic transition assignments of Sethuraman *et al.* [Ref. 20(b)] for $2_0^1 4_0^3$ and that of Apel and Lee (Refs. 17 and 24) for $2_0^1 4_0^1 6_0^1$ are used.

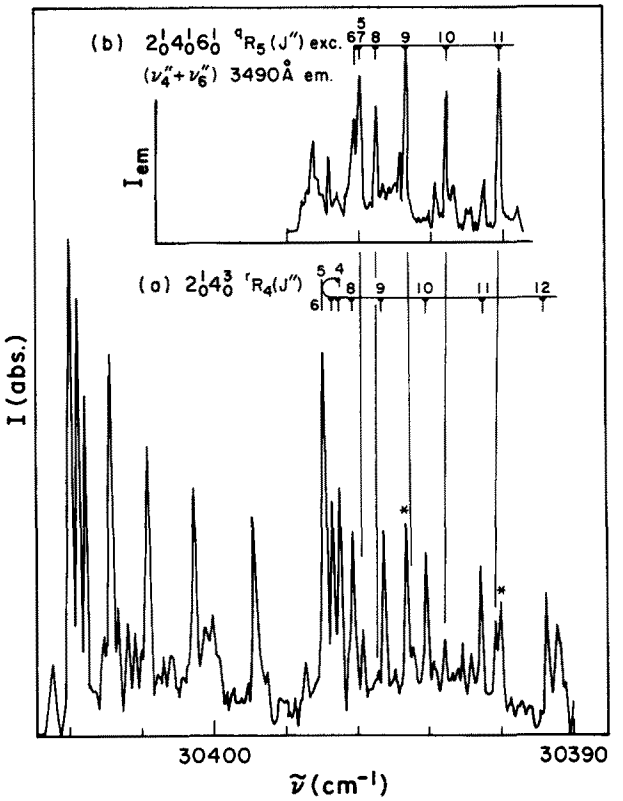

FIG. 3. A comparison of an FT absorption spectrum in the $^rR_4(J'')$ region of the $2_0^1 4_0^3$ transition (a, lower panel, courtesy of Ramsay and Neil) and an RELFEX spectrum of the emission locked onto the ^pP transition terminating on the ($\nu_4'' + \nu_6''$) level at 3578 Å with an 8 Å bandpass (b, upper panel)—a fingerprint of the $2_0^1 4_0^1 6_0^1$ transition. The two peaks with an asterisk are $^rR_5(14)$ and $^rR_5(15)$ of $2_0^1 4_0^3$ from left to right.

tion must be exercised in using the observed line intensities associated with pulsed laser excitation for any quantitative interpretation. Although all of the rotational structures observed in the absorption spectrum [Fig. 2(a)] are present in the FEX spectrum [Fig. 2(b)], the region of the $2_0^1 4_0^3 {}^rR_5$ and $^rR_4$ subbands of the latter is more congested due to the presence of some additional lines (see below). On the other hand, the RELFEX spectrum shown in Fig. 2(c) which monitors the emission terminating on the $v_2'' = 1$ rovibrational levels of the ground electronic state is nearly identical to the absorption spectrum shown in Fig. 2(a). The appearance of the forbidden $2_0^1 4_0^1 6_0^1$ subband first reported by Sethuraman *et al.*[20(a)] was verified recently with the observation of the RELFEX subband for which we gave a preliminary rotational assignment.[17] Some of the congestion features that cannot be attributed to the $^rR_4(J'')$ and $^rR_5(J'')$ subbands of the $2_0^1 4_0^3$ rovibronic transition may be attributed, however, to the $^qR_5(J'')$ subband of the $2_0^1 4_0^1 6_0^1$ transition. This is illustrated by the comparison of the RELFEX spectrum, "locked onto" the ^pP-subband emission to the $4_1 6_1$ level,[17] with the overlapping $2_0^1 4_0^3 {}^rR_4(J'')$ subband absorption spectrum in Fig. 3. The observed frequencies for the $^qR_5(J'')$ transitions are listed in Table II.

B. Fluorescence emission spectra

The fluorescence emission spectra from the rotational levels of the $2^1 4^3$ and $2^1 4^1 6^1$ vibrational levels were recorded mainly in the 3420–3590 Å region which covers the E''_{vib} = 1100–2500 cm^{-1} range, $v_4'' = 1$ to $v_6'' = 2$. This region provides relatively unambiguous information about the rovi-

TABLE II. Observed and calculated frequencies ($\tilde{\nu}$) for rovibronic transitions in the $2_0^1 4_0^1 6_0^1 {}^qR_5(J'')$ subband.

Rotational transition	Observed $\tilde{\nu}_{exc}$ (cm^{-1})	Calculated[a] $\tilde{\nu}_{abs}$ (cm^{-1})	$\Delta\tilde{\nu}$ (obs − calc) (cm^{-1})
$^qR_5(5)$	30 396.01	30 395.97	− 0.04
$^qR_5(6)$	30 396.16	30 396.15	0.01
$^qR_5(7)$	30 396.01	30 396.02	− 0.01
$^qR_5(8)$	30 395 54	30 395.56	− 0.02
$^qR_5(9)$	30 394.74	30 394.78	− 0.04
$^qR_5(10)$	30 393.66	30 393.68	− 0.02
$^qR_5(11)$	30 392.29	30 392.25	0.04

[a] The calculated values were obtained using the vibronic origin of 30 395.0 cm^{-1} (Ref. 24), the free-jet data (Ref. 24), and the rotational constants listed in Table III.

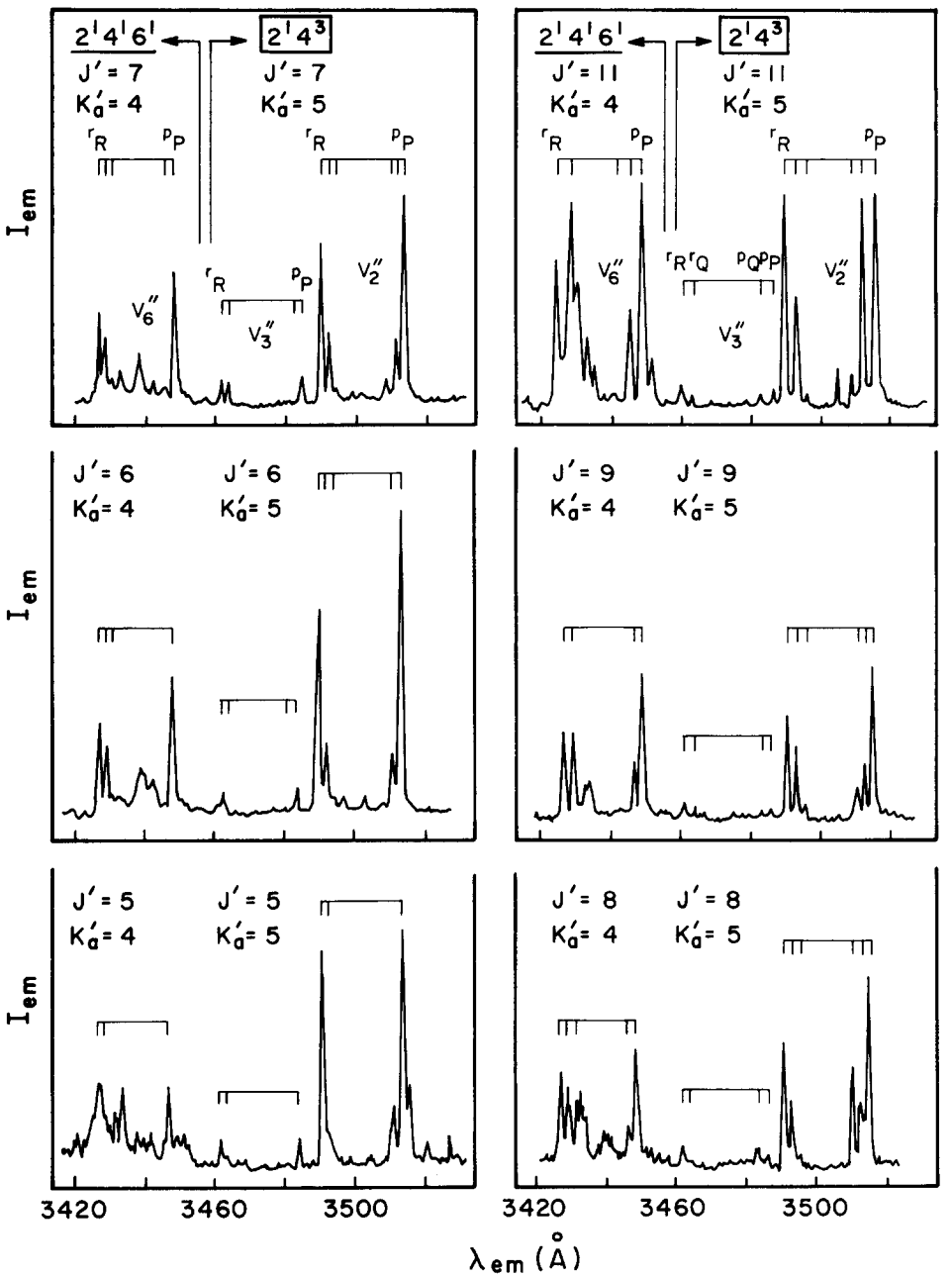

FIG. 4. Fluorescence emission spectra from a set of $2^1 4^3$ $K_a' = 5$ rotational levels ($J' = 5$–11) pumped by the $2_0^1 4_0^3 {}^rR_4(J'')$ transitions (30 396.58–30 397.17 cm^{-1}) for $J'' = 4$–10. H_2CO pressure was 400 mTorr and the monochromator bandpass was 1.0 Å.

brational identities of the emitting states of interest. Fluorescence emission spectra from a set of $2^1 4^3$ $K_a' = 5$ rotational levels ($J' = 5$–11) pumped by the appropriate $2_0^1 4_0^3 {}^rR_4(J'')$ transitions are shown in Fig. 4. The fluorescence emission spectra from the $J' = 8$, $K_a' = 5$ level prepared by the $^pP_6$ (9) transition is shown in Fig. 5. A comparison of this spectrum with the spectrum of the $J' = 8$, $K_a' = 5$ level pumped by the $^rR_4$ (7) transition in Fig. 4 verifies that the former is considerably "cleaner" than the latter. This indicates that the preparation of the $2^1 4^3$ $J' = 8$, $K_a' = 5$ level by the $^pP_6$ (9) excitation is appreciably purer than that by the $^rR_4$ (7) excitation. Such a comparison provides a useful test of uncontaminated excitation. The fact that a Coriolis resonance occurs for the $2^1 4^3$ $K_a' = 5$ manifold is shown in Fig. 6 as indicated by the strong appearance of the ν_6'' rotational transitions. The vibrational level energies and the rotational constants which were used to assign the rovibrational transitions are summarized in Table III. Fluorescence emission spectra from a set of the $2^1 4^1 6^1$ $K_a' = 5$ rotational levels ($J' = 7$–11) pumped by the appropriate $2_0^1 4_0^1 6_0^1 {}^qR_5(J'')$ transitions are shown in Fig. 7. The emissions in the 3640–3670 Å region to $2_1 6_1$ rovibrational levels from the $J' = 10$ and 11 levels are shown in Fig. 8.

The assignment of the observed rovibrational bands, in both excitation and emission, was aided by comparison with the computed rotational band contours calculated with an asymmetric rotor program using the molecular constants given in Table III.[25–30] The fit of the calculated transition frequencies to the observed emission frequencies is tabulated in Tables IV–VII. The agreement is satisfactory in most cases within the probable experimental error of ~ 8 cm^{-1}, the monochromator bandpass/wavelength drive accuracy. The rovibrational emission intensities were also calculated using the zero-order vibronic transition oscillator strengths

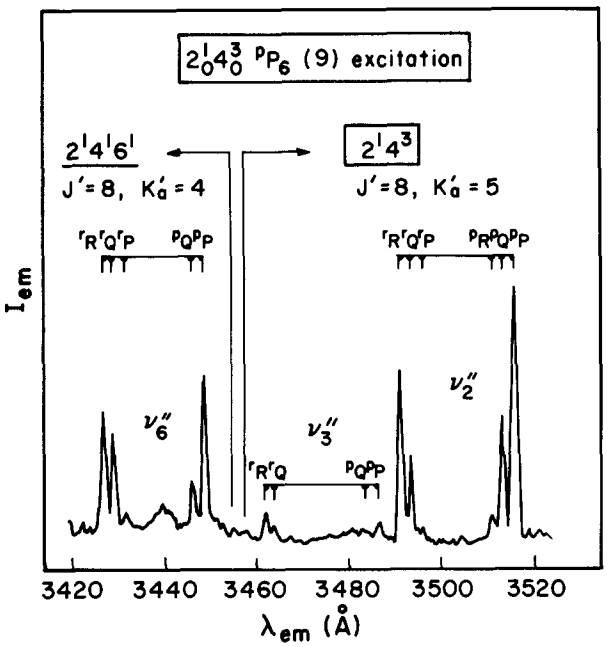

FIG. 5. Fluorescence emission spectra from the $2^1 4^3$ $J'=8$, $K_a'=5$ level prepared by the $2_0^1 4_0^3 {}^pP_6(9)$ transition at 30 192.46 cm^{-1}.

predicted by the *ab initio* CI calculations of van Dijk *et al.*[31] The calculated fluorescence intensities are shown in Fig. 9 for the 3 rotational levels of $2^1 4^3$ observed in Fig. 6. The agreement between experiment and theory is satisfactory, except for the $2\nu_4''$ emission which is observed to be weaker than expected but more importantly it shows the suppression of the *p*-form subbands.

C. $2_0^1 6_0^1$ band

We have recorded FEX and RELFEX spectra of the *p*-form transition region of the $2_0^1 4_0^3$ and $2_0^1 6_0^1$ bands in the $K_a''=2$–5 manifolds. Due to lack of space, these spectra will not be shown here, and the results of the rotational analysis will be published elsewhere.[30] One important result of interest here is that the $2^1 6^1$ $K_a'=0$–4 levels are a little perturbed by Coriolis interaction, since the vibrational origin of $2^1 6^1$ is 88 cm^{-1} below the $2^1 4^3$ origin and 143 cm^{-1} below the $2^1 4^1 6^1$ origin; these vibrational energy gaps are too large to give strong Coriolis interactions at $K_a'=0$–4.

IV. DISCUSSION

All of the emission experiments were done at pressures equal to or less than 400 mTorr of H_2CO. If a gas kinetic collision cross section of 63 $Å^2$ is assumed, the mean time between such collisions at 400 mTorr is 190 ns. Rotational energy transfer under favorable conditions, particularly for ΔJ collisions of H_2CO (S_1)[32] or D_2CO (S_0),[33] can have a cross section of ~ 300 $Å^2$. If a value of 300 $Å^2$ is used as the maximum value of the rotational energy transfer cross section, the mean time between such collisions at 400 mTorr is 40 ns. This is at least twice as long as the S_1 lifetimes of the $2^1 4^3$ rovibrational levels of interest here.[24] The lifetimes of the $2^1 4^1 6^1$ rovibrational levels are not known but are probably comparable to those of $2^1 4^1$ rovibrational levels. Therefore, we should expect that most of the $2^1 4^3$ and $2^1 4^1 6^1$ species giving rise to the observed fluorescence emission are collision-free with respect to rotational relaxation as well as vibrational and electronic relaxation, the latter being considerably less efficient than rotational relaxation in S_1 H_2CO. In the present study, as well as in the previous study of the 5^1 and $1^1 4^1$ rotational levels,[16] there is no compelling evidence of rotational relaxation for the emitting species as manifested in the dispersed emission spectra. Therefore, we shall proceed with the discussion without further consideration of collision-induced processes; this is an area of interest which deserves an investigation in the future.

A. Absorption and fluorescence excitation

Knowledge of the vibronic oscillator strengths (f's) of the optical transitions that connect the S_1 vibronic states (shown in Fig. 1) with the S_0 ground vibrational state is necessary for modeling the electronic absorption spectrum. For the vibronically allowed dipole transitions of moderate intensity in H_2CO (*B* and *C*-type bands), we can obtain numerical results of f-values from the *ab initio* CI calculation performed by van Dijk *et al.*[31] These are given in Table VIII for the emission transitions of interest. The *A*-type bands are two orders of magnitude weaker, and for these the calcula-

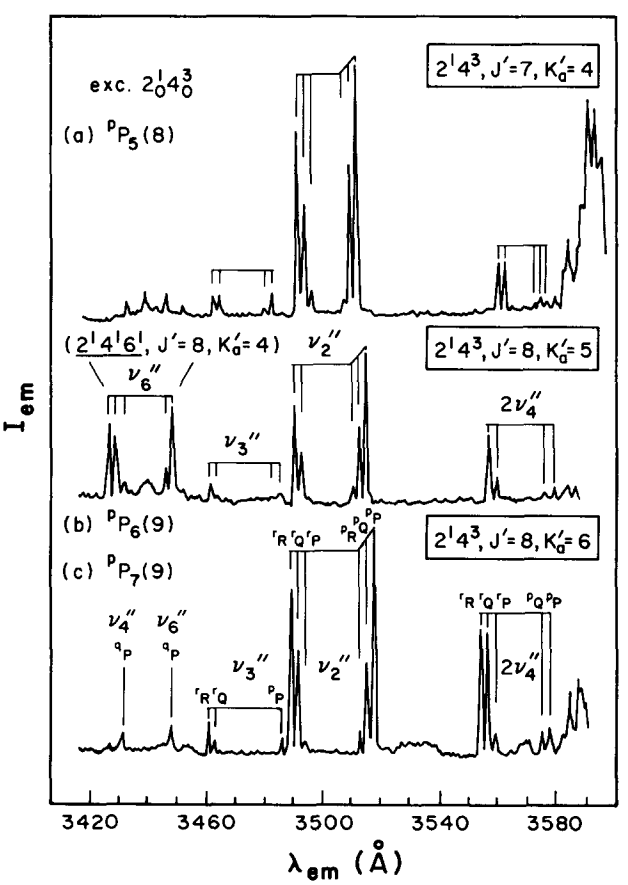

FIG. 6. A comparison of the fluorescence emission spectra from three of the $2^1 4^3$ rotational levels belonging to three different K_a' manifolds: (a) the $J'=7$, $K_a'=4$ level pumped by the $^pP_5(8)$ transition at 30 222.44 cm^{-1}; (b) the $J'=8$, $K_a'=5$ level pumped by the $^pP_6(9)$ transition at 30 192.46 cm^{-1}; (c) the $J'=8$, $K_a'=6$ level pumped by the $^pP_7(9)$ transition at 30 167.47 cm^{-1}.

TABLE III. Vibrational energies and rotational constants of the ground and excited electronic states (in cm^{-1}).

Level	G_0	A	B	C	Ref.
			$H_2CO\ \tilde{X}\ ^1A_1$		
4_1	1167.26	9.289 0	1.287 243	1.135 716	19, 25[a]
6_1	1249.09	9.488 1	1.298 244	1.129 886	19, 25[a]
3_1	1500.18	9.466 97	1.300 078	1.129 318	19
2_1	1746.01	9.399 91	1.287 901 4	1.125 396 1	19, 26[b]
4_2	2328.9	~7.7	G.S.[c]	G.S.[c]	27[d]
4_16_1	(2413.2)[e]	9.39[f]	G.S.[c]	G.S.[c]	28[e,g]
6_2	(2498)[h]	...	...	...	
2_16_1	3000.07				29
			$H_2CO\ \tilde{A}\ ^1A_2 (T_{00} = 28\ 188.0\ cm^{-1})$		
2^16^1	2064.2	9.2203	1.117 2	0.992 0	24, 30
2^14^3	2152.0	8.2162	1.105 29	1.010 97	19, 21, $K_a = 0$–4
$2^14^16^1$	2207.0	8.960(9)	1.106(37)	1.004(39)	24, $K_a = 5$ (Table II)

[a] The rovibrational energies actually observed were used, since 3_1, 4_1, and 6_1 levels are the Coriolis triad.
[b] The rovibrational energies actually observed were used.
[c] The ground state values as given in Ref. 19 ($A_0 = 9.405\ 526\ cm^{-1}$; $B_0 = 1.295\ 431\ cm^{-1}$; $C_0 = 1.134\ 191\ cm^{-1}$) were used to guess a value of $\bar{B} = 1.2148\ cm^{-1}$.
[d] A Coriolis triad (4_2, 4_16_1, and 6_2) was assumed as in Refs. 16 and 27.
[e] The value of $E''_v(4_16_1)$ was calculated using vibrational constants obtained from Ref. 28.
[f] The A'' value for 4_16_1 was assumed.
[g] The rovibrational energies of 4_16_1 were calculated from the expression, $E''_{v,r} = E''_v(4_16_1) + E''_r(4_16_1, J, K_a)$.
[h] Estimated as $2\times\nu''_6$.

tion is considerably more difficult. The results for the B- and C-type absorption transitions of interest are summarized in Table IX. Clearly, the $2_0^14_0^3$ band with $\mathbf{f} = 8.7\times10^{-6}$ is predicted to be the strongest in the $E'_{vib} = 1800$–$2300\ cm^{-1}$ region, in agreement with the observation. The next stron-

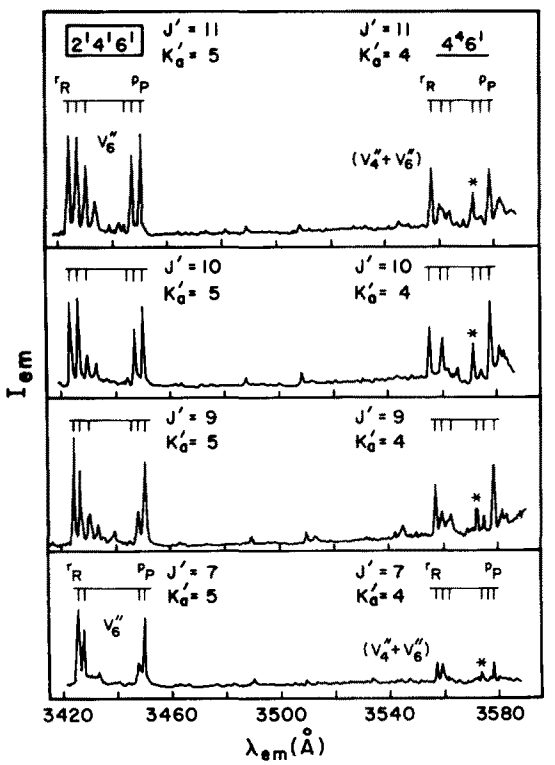

FIG. 7. Fluorescence emission spectra from a set of $2^14^16^1$ $K'_a = 5$ rotational levels ($J' = 7$, 9, 10, and 11) pumped by the $2_0^14_0^16_0^1\,{}^qR_5(J'')$ transitions (30 396.16–30 393.66 cm^{-1}, see Table II) for $J'' = 6$, 8, 9, and 10. H_2CO pressure was 400 mTorr and the monochromator bandpass was 1.0 Å. Since the ${}^qR_5(5)$ and ${}^qR_5(7)$ lines overlap [see Fig. 3(b)], they were not used to produce wavelength-dispersed emission.

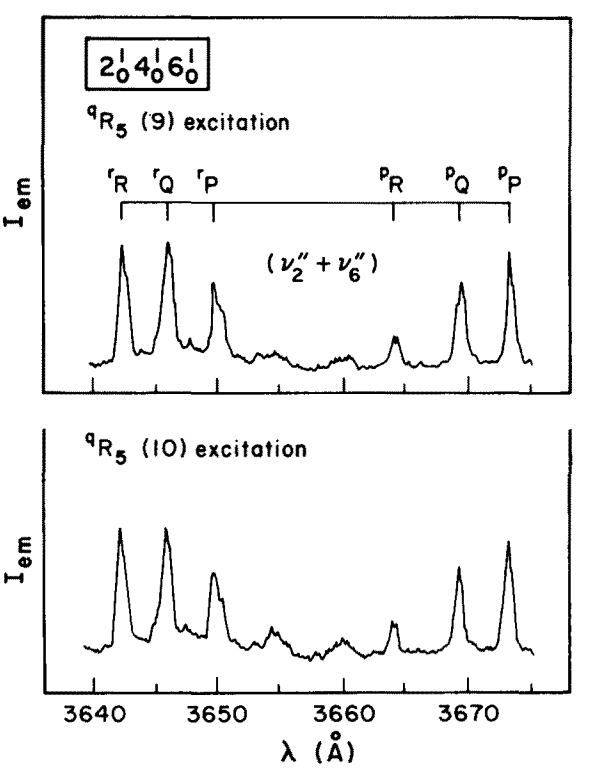

FIG. 8. The fluorescence emission bands terminating on 2_16_1 rovibrational levels from two $2^14^16^1$ $K'_a = 5$ rovibrational levels pumped by the ${}^qR_5(9)$ and ${}^qR_5(10)$ transitions. The conditions are the same as in Fig. 7.

TABLE IV. Observed and calculated frequencies for fluorescence emission from $2^1 4^1 6^1$ ($K' = 5$) SRL's to the ν_6'' and ($\nu_2'' + \nu_6''$) levels.

Pump trans.	Lower vibr.[a,b]	Upper J'	Upper K_a'	Lower J''	Lower K_a''	$\tilde{\nu}$ (cm^{-1}) obs	$\tilde{\nu}$ (cm^{-1}) calc
$^qR_6(6)$	ν_6''	7	5	6	4	29 197	29 203
				7	4	29 177	29 186
				8	4	29 158	29 167
				6	6	...	29 024
				7	6	29 009	29 007
				8	6	28 989	28 988
$^qR_5(8)$	ν_6''	9	5	8	4	29 199	29 203
				9	4	29 177	29 181
				10	4	29 151	29 157
				8	6	...	29 024
				9	6	28 998	29 002
				10	6	28 975	28 978
	$\nu_2'' + \nu_6''$	9	5	8	4	27 457	27 456
				9	4	27 435	27 434
				10	4	27 403	27 410
				8	6	...	27 279
				9	6	27 258	27 258
				10	6	27 235	27 233
$^qR_5(9)$	ν_6''	10	5	9	4	29 199	29 202
				10	4	29 175	29 178
				11	4	29 148	29 151
				9	6	29 022	29 023
				10	6	28 995	28 999
				11	6	28 969	28 972
	$\nu_2'' + \nu_6''$	10	5	9	4	27 455	27 455
				10	4	27 430	27 431
				11	4	27 396	27 405
				9	6	27 278	27 278
				10	6	27 254	27 254
				11	6	27 227	27 228
$^qR_5(10)$	ν_6''	11	5	10	4	29 198	29 201
				11	4	29 171	29 174
				12	4	29 144	29 145
				10	6	29 037	29 022
				11	6	28 992	28 996
				12	6	28 964	28 967
	$\nu_2'' + \nu_6''$	11	5	10	4	27 454	27 454
				11	4	27 428	27 428
				12	4	27 398	27 399
				10	6	...	27 278
				11	6	27 253	27 251
				12	6	27 223	27 222
$^qR_5(11)$	ν_6''	12	5	11	4	29 201	29 200
				12	4	29 172	29 171
				13	4	29 141	29 139
				11	6	29 020	29 021
				12	6	28 992	28 992
				13	6	28 961	28 961

TABLE V. Observed and calculated frequencies for fluorescence emission from the $4^4 6^1$ *zero-order* components of the mixed eigenstate of $2^1 4^1 6^1$ parentage.

Pump trans.	Lower vibr.[a]	Upper J'	Upper K_a'	Lower J''	Lower K_a''	$\tilde{\nu}$ (cm^{-1}) obs	$\tilde{\nu}$ (cm^{-1}) calc
$^qR_5(6)$	$\nu_4'' + \nu_6''$	7	4	6	3	28 122	28 114
				7	3	28 094	28 097
				8	3	28 073	28 077
				6	5	27 989	27 983
				7	5	27 975	27 966
				8	5	27 939	27 947
$^qR_5(8)$	$\nu_4'' + \nu_6''$	9	4	8	3	28 105	28 110
				9	3	28 085	28 088
				10	3	28 061	28 064
				8	5	27 983	27 979
				9	5	27 962	27 957
				10	5	27 935	27 933
$^qR_5(9)$	$\nu_4'' + \nu_6''$	10	4	9	3	28 106	28 109
				10	3	28 071	28 085
				11	3	...	28 058
				9	5	27 984	27 978
				10	5	27 961	27 954
				11	5	27 932	27 927
$^qR_5(10)$	$\nu_4'' + \nu_6''$	11	4	10	3	28 105	28 108
				11	3	28 079	28 081
				12	3	...	28 052
				10	5	27 984	27 977
				11	5	27 956	27 951
				12	5	27 932	27 922
$^qR_5(11)$	$\nu_4'' + \nu_6''$	12	4	11	3	28 108	28 110
				12	3	28 086	28 080
				13	3	28 048	28 049
				11	5	27 987	27 979
				12	5	27 937	27 950
				13	5	27 928	27 918

gest transitions are expected to be the $2_0^1 6_0^1$ and 4_0^5 bands with $f = 1.8 \times 10^{-6}$ and $f = 1.5 \times 10^{-6}$, respectively, which are about 5–6 times weaker than the $2_0^1 4_0^3$ band. $f(3_0^1 4_0^3)$ is about 10 times weaker than $f(2_0^1 4_0^3)$, and $f(3_0^1 6_0^1)$ and $f(4_0^4 6_0^1)$ are ~50 times weaker. Therefore, it is not surprising that we were able to record an RELFEX spectrum of the $2_0^1 6_0^1$ band[30] but were unable to find the 4_0^5 and $4_0^4 6_0^1$ bands even by free-jet/fluorescence spectroscopy. It is probable that the relatively low f values as well as the very short S_1 lifetimes (due to more rapid predissociation making Φ_f small) of 4^5 and $4^4 6^1$ combine to make fluorescence detection very difficult. Of course, the fact[24] that the S_1 lifetime of $2^1 6^1$ is longer than that of $2^1 4^3$ by a factor of 4–5 certainly enhanced the detection of the $2_0^1 6_0^1$ band and allowed us to use the rovibronic emission-locked fluorescence excitation technique,[17,30] as mentioned in Sec. III C. We expect that the 4^5 levels have a significantly shorter S_1 lifetime than the $2^1 6^1$ levels,[34] and therefore, the detection of the 4_0^5 band by the RELFEX technique may be considerably more difficult. The detection of the $3_0^1 6_0^1$ and $4_0^4 6_0^1$ bands should be even more difficult.

The region of the $2_0^1 4_0^3 {}^rR_4(J'')$ excitation and the $2_0^1 4_0^1 6_0^1 {}^qR_5(J'')$ excitation shall now be considered for discussion. Most of the relatively strong absorption lines observed between 30 397 and 30 391 cm^{-1} have been attributed to the $2_0^1 4_0^3$ transition, as labeled in Fig. 3. Four of the weaker absorption lines [by a factor of ~10 as compared to the $2_0^1 4_0^3 {}^rR_5(J'')$ lines] in this region occur at similar excitation frequencies of the $2_0^1 4_0^1 6_0^1 {}^qR_5$ lines with $J' = 5 + 7, 8, 9, 10$, and 11 [see Fig. 3(b)]. This result can then be interpreted to mean that an appreciable percentage of another zero-order component of $\mathbf{b}_2$ (or $\mathbf{b}_1$) symmetry ($K_a' = 4$ or 6) is

TABLE VI. Observed and calculated frequencies for emission from the $2^1 4^3$ $K'_a = 4$, 5, and 6 levels.

Pump trans.	Lower vibr.	Upper J'	Upper K'_a	Lower J''	Lower K''_a	$\tilde{\nu}$ (cm^{-1}) obs	$\tilde{\nu}$ (cm^{-1}) calc
$^pP_5(8)$	ν''_6	7	4	6	4	...	29 066
				7	4	...	29 049
				8	4	29 029	29 030
	ν''_3	7	4	6	3	28 889	28 889
				7	3	28 870	28 872
				8	3	...	28 852
				6	5	...	28 757
				7	5	28 741	28 740
				8	5	28 721	28 720
	ν''_2	7	4	6	3	28 643	28 644
				7	3	28 626	28 627
				8	3	28 605	28 608
				6	5	28 512	28 513
				7	5	28 496	28 496
				8	5	28 475	28 477
	$2\nu''_4$	7	4	6	3	28 084	28 084
				7	3	28 069	28 069
				8	3	...	28 053
				6	5	27 976	27 972
				7	5	27 958	27 955
				8	5	27 938	27 936
$^pP_5(10)$	ν''_4	9	4	8	4	29 186	29 183
				9	4	...	29 161
				10	4	29 137	29 137
	ν''_6	9	4	8	4	29 067	29 066
				9	4	...	29 044
				10	4	29 018	29 020
	ν''_3	9	4	8	3	28 885	28 888
				9	3	28 866	28 866
				10	3	...	28 842
				8	5	...	28 756
				9	5	28 733	28 734
				10	5	28 709	28 710
	ν''_2	9	4	8	3	28 643	28 644
				9	3	28 621	28 622
				10	3	28 596	28 598
				8	5	28 509	28 513
				9	5	28 488	28 491
				10	5	28 466	28 467
	$2\nu''_4$	9	4	8	3	28 078	28 091
				9	3	28 054	28 073
				10	3	...	28 053
				8	5	...	27 974
				9	5	...	27 952
				10	5	...	27 928
$^pP_5(11)$	ν''_4	10	4	9	4	...	29 182
				10	4	...	29 158
				11	4	29 131	29 131
	ν''_6	10	4	9	4	29 066	29 065
				10	4	...	29 041
				11	4	29 015	29 014
	ν''_3	10	4	9	3	28 888	28 887
				10	3	28 864	28 863
				11	3	...	28 836
				9	5	...	28 756
				10	5	28 730	28 731
				11	5	28 705	28 704
	ν''_2	10	4	9	3	28 643	28 643
				10	3	28 618	28 619
				11	3	28 591	28 596
				9	5	28 512	28 512
				10	5	28 488	28 488
				11	5	28 462	28 462
$^pP_6(7)$	ν''_3	6	5	5	4	28 899	28 896

TABLE VI. (*continued.*)

Pump trans.	Lower vibr.	Upper J'	Upper K'_a	Lower J''	Lower K''_a	$\tilde{\nu}$ (cm^{-1}) obs	$\tilde{\nu}$ (cm^{-1}) calc
				6	4	28 872	28 881
				7	4	...	28 864
				6	6	...	28 717
				7	6	28 704	28 700
	ν''_2	6	5	5	4	28 652	28 651
				6	4	28 635	28 637
				7	4	...	28 620
				6	6	28 474	28 473
				7	6	28 458	28 457
	$2\nu''_4$	6	5	5	4	28 098	28 097
				6	4	28 067	28 083
				7	4	...	28 066
				6	6	...	27 953
				7	6	27 922	27 936
$^pP_6(8)$	ν''_3	7	5	6	4	28 895	28 896
				7	4	28 877	28 879
				8	4	...	28 859
				6	6	...	28 732
				7	6	...	28 714
				8	6	28 698	28 695
	ν''_2	7	5	6	4	28 652	28 652
				7	4	28 633	28 634
				8	4	28 615	28 615
				6	6	28 498	28 488
				7	6	28 472	28 471
				8	6	28 452	28 452
	$2\nu''_4$	7	5	6	4	28 097	28 097
				7	4	28 071	28 080
				8	4	...	28 061
				6	6	...	27 967
				7	6	...	27 951
				8	6	...	27 931
$^pP_6(9)$	ν''_3	8	5	7	4	28 893	28 896
				8	4	28 877	28 876
				9	4	...	28 854
				7	6	...	28 731
				8	6	28 711	28 712
				9	6	28 691	28 690
	ν''_2	8	5	7	4	28 652	28 651
				8	4	28 630	28 632
				9	4	28 611	28 610
				7	6	28 486	28 488
				8	6	28 468	28 469
				9	6	28 446	28 447
	$2\nu''_4$	8	5	7	4	28 098	28 095
				8	4	28 074	28 076
				9	4	...	28 054
				7	6	...	27 966
				8	6	27 947	27 947
				9	6	27 906	27 925
$^pP_6(10)$	ν''_3	9	5	8	4	28 898	28 895
				9	4	28 876	28 873
				10	4	...	28 848
				8	6	...	28 781
				9	6	28 716	28 709
				10	6	28 686	28 684
	ν''_2	9	5	8	6	28 651	28 651
				9	6	28 629	28 629
				10	6	28 603	28 605
				8	6	28 486	28 488
				9	6	28 465	28 466
				10	6	28 444	28 442
$^pP_7(9)$	ν''_4	8	6	7	6	...	29 182
				8	6	29 163	29 162
				9	6	...	29 140

TABLE VI. (*continued.*)

Pump trans.	Lower vibr.	Upper J'	Upper K'_a	Lower J''	Lower K''_a	$\tilde{\nu}$ (cm^{-1}) obs	$\tilde{\nu}$ (cm^{-1}) calc
$^pP_7(9)$	ν_6''	8	6	7	6	...	29 032
				8	6	29 025	29 013
				9	6	...	28 991
	ν_3''	8	6	7	5	28 901	28 902
				8	5	28 882	28 883
				9	5	...	28 861
				7	7	...	28 706
				8	7	28 686	28 686
				9	7	...	28 664
	ν_2''	8	6	7	5	28 659	28 658
				8	5	28 639	28 639
				9	5	28 618	28 617
				7	7	28 462	28 463
				8	7	28 444	28 444
				9	7	28 422	28 422
	$2\nu_4''$	8	6	7	5	28 118	28 117
				8	5	28 099	28 098
				9	5	28 074	28 076
				7	7	...	27 962
				8	7	27 938	27 942
				9	7	27 918	27 920
$^pP_7(10)$	ν_6''	9	6	8	6	29 031	29 032
				9	6	29 009	29 010
				10	6	...	28 986
	ν_3''	9	6	8	5	28 902	28 902
				9	5	28 880	28 880
				10	5	...	28 855
				8	7	...	28 705
				9	7	28 686	28 683
				10	7	...	28 659
	ν_2''	9	6	8	5	28 661	28 658
				9	5	28 638	28 636
				10	5	...	28 612
				8	7	28 461	28 463
				9	7	28 442	28 441
				10	7	28 420	28 417
	$2\nu_4''$	9	6	8	5	28 120	28 119
				9	5	28 098	28 097
				10	5	28 077	28 073
				8	7	...	27 963
				9	7	27 936	27 942
				10	7	27 913	27 918
$^rR_4(4)$	ν_3''	5	5	4	4	28 896	28 895
				5	4	...	28 883
				6	4	...	28 869
				6	6	28 705	28 704
	ν_2''	5	5	4	4	28 651	28 651
				5	4	28 640	28 639
				6	4	...	28 625
				6	6	28 461	28 461
	$2\nu_4''$	5	5	4	4	28 096	28 095
				5	4	28 067	28 083
				6	4	...	28 068
				6	6	...	27 939
$^rR_4(9)$	ν_3''	10	5	9	4	28 898	28 894
				10	4	28 870	28 870
				11	4	...	28 843
				9	6	...	28 730
				10	6	...	28 705
				11	6	...	28 678
$^rR_4(9)$	ν_2''	10	5	9	4	28 648	28 650
				10	4	28 624	28 626
				11	4	...	28 600
				9	6	28 482	28 487
				10	6	28 458	28 463

TABLE VI. (*continued.*)

Pump trans.	Lower vibr.	Upper J'	Upper K'_a	Lower J''	Lower K''_a	$\tilde{\nu}$ (cm^{-1}) obs	$\tilde{\nu}$ (cm^{-1}) calc
				11	6	28 431	28 436
	$2\nu_4''$	10	5	9	4	28 094	28 094
				10	4	28 067	28 069
				11	4	...	28 043
				9	6	...	27 965
				10	6	...	27 940
				11	6	...	27 914
$^rR_4(10)$	ν_3''	11	5	10	4	28 894	28 896
				11	4	28 865	28 869
				12	4	...	28 840
				10	6	...	28 731
				11	6	28 704	28 705
				12	6	28 671	28 675
	ν_2''	11	5	10	6	28 649	28 652
				11	6	28 622	28 626
				12	6	28 593	28 596
				10	4	28 485	28 489
				11	4	28 459	28 462
				12	4	28 430	28 434
$^rR_4(11)$	ν_3''	12	5	11	4	28 894	28 891
				12	4	28 862	28 862
				13	4	...	28 830
				11	6	...	28 727
				12	6	28 697	28 698
				13	6	28 666	28 666
	ν_2''	12	5	11	4	28 646	28 648
				12	4	28 617	28 619
				13	4	28 586	28 587
				11	6	28 486	28 485
				12	6	28 456	28 456
				13	6	28 423	28 424
	$2\nu_4''$	12	5	11	4	28 092	28 091
				12	4	28 067	28 062
				13	4	...	28 030
				11	6	...	27 962
				12	6	...	27 933
				13	6	...	27 901

mixed into the $2^1 4^1 6^1$ zero-order parent ($K'_a = 5$) by **b**-axis (or **c**-axis) Coriolis coupling, since the $2_0^1 4_0^1 6_0^1$ transition (vibronically allowed A type) should be extremely weak.[35]

The fluorescence excitation intensity of the $2_0^1 4_0^1 6_0^1$ band was found to be about 10–20 times weaker than that of the $2_0^1 4_0^3$ band for jet-cooled H_2CO (see Fig. 1 of Ref. 24). However, the fluorescence excitation intensities of the $2_0^1 4_0^1 6_0^1 {}^qR_5(J'')$ lines are comparable to those of the $2_0^1 4_0^3 {}^rR_4(J'')$ lines as shown in Fig. 3, whereas the other ${}^qR_{K'}(J'')$ subbands are not clearly observable. These two observations support the conclusion that the $2_0^1 4_0^1 6_0^1 {}^qR_5(J'')$ lines are enhanced compared to other $2_0^1 4_0^1 6_0^1 {}^qR_{K'}(J'')$ lines. Fortunately, the strong enhancement of the ${}^qR_5(J'')$ transition (by a factor of 10–20) can be explained theoretically[16,18] by invoking Coriolis-induced intensity borrowing from a near-resonant strong transition. An example of this type of intensity borrowing was found by Kerr and Ramsay;[35] the 3_0^1 q-form band appears through Coriolis interaction of 3^1 with $2^1 4^1$.

A set of rotational constants for $2^1 4^1 6^1$ was determined earlier from 11 rotational transitions observed with jet-

TABLE VII. Observed and calculated frequencies for fluorescence emission to the ν_6'' level from the $K_a' = 4$ level of the $2^1 4^1 6^1$ *zero-order* component of the mixed eigenstate of $2^1 4^3$ parentage.

Pump trans.	Lower vibr.	Upper J'	Upper K_a'	Lower J''	Lower K_a''	$\tilde{\nu}$ (cm^{-1}) obs	$\tilde{\nu}$ (cm^{-1}) calc
$^pP_6(7)$	ν_6''	6	4	5	3	29 197	29 195
				6	3	29 182	29 180
				7	3	29 169	29 163
				7	5	29 020	29 018
$^pP_6(8)$	ν_6''	7	4	6	3	29 191	29 195
				7	3	29 174	29 178
				8	3	29 163	29 158
				8	5	29 012	29 013
$^pP_6(9)$	ν_6''	8	4	7	3	29 194	29 195
				8	3	29 175	29 175
				9	3	29 152	29 153
				8	5	29 028	29 030
				9	5	29 009	29 008
$^rR_4(4)$	ν_6''	5	4	4	3	29 198	29 194
				5	3	29 181	29 182
				6	5	29 023	29 022
$^rR_4(7)$	ν_6''	8	4	7	3	29 196	29 195
				8	3	29 176	29 175
				9	3	29 150	29 153
				8	5	29 025	29 030
				9	5	29 010	29 008
$^rR_4(8)$	ν_6''	9	4	8	3	29 200	29 194
				9	3	29 173	29 172
				10	3	29 152	29 147
				9	5	29 026	29 027
				10	5	29 004	29 003
$^rR_4(10)$	ν_6''	11	4	10	3	29 193	29 195
				11	3	29 164	29 168
				12	3	29 147	29 139
				11	5	29 019	29 024
				12	5	28 994	28 994

TABLE VIII. Calculated oscillator strengths (**f**) for emission from various *zero-order* S_1 H_2CO vibronic levels.

Vibronic transition	Band type	Transition[a] energy (cm^{-1})	Oscillator strength (**f**)[c]
		$2^1 6^1$ (b_2)	
$2_0^1 4_1^0 6_0^1$ [d]	*A*	29 084	...
$2_0^1 6_1^1$	*A*	29 003	...
$2_0^1 3_1^0 6_0^1$	*C*	28 752	3.18(−7)
$2_1^1 6_0^1$	*C*	28 506	1.48(−6)
$2_0^1 4_2^0 6_0^1$	*C*	27 925	9.36(−7)
$2_0^1 4_1^0 6_1^1$	*B*	27 839[b]	3.63(−5)
$2_0^1 6_2^1$	*C*	27 754	4.75(−6)
		$2^1 4^3$ (b_1)	
$2_0^1 4_1^3$	*A*	29 173	...
$2_0^1 4_0^3 6_1^0$ [d]	*A*	29 091	...
$2_0^1 3_1^0 4_0^3$	*B*	28 840	1.51(−6)
$2_1^1 4_0^3$	*B*	28 594	7.09(−6)
$2_0^1 4_2^3$	*B*	28 013	1.28(−5)
$2_0^1 4_1^3 6_1^0$	*C*	27 927[b]	1.73(−6)
$2_0^1 4_0^3 6_2^0$	*B*	27 842	8.11(−8)
		$3^1 6^1$ (b_2)	
$3_1^1 6_0^1$	*C*	28 885	~8(−7)
$3_0^1 4_1^0 6_1^1$	*B*	27 951	3.48(−6)
		$2^1 4^1 6^1$ (a_2)	
$2_0^1 4_1^1 6_0^1$	*C*	29 228	1.34(−6)
$2_0^1 4_0^1 6_1^1$	*B*	29 146	6.90(−6)
$2_1^1 4_0^1 6_0^1$ [d]	*A*	28 649	...
$2_0^1 4_2^1 6_0^1$ [d]	*A*	28 068	...
$2_0^1 4_1^1 6_1^1$	*A*	27 982[b]	...
$2_0^1 4_0^1 6_2^1$ [d]	*A*	27 897	...
		$3^1 4^3$ (b_1)	
$3_1^1 4_0^3$	*B*	28 929	~4(−6)
		$4^4 6^1$ (b_2)	
$4_1^4 6_1^1$	*B*	28 101	<5(−7)[e]

[a] Transition energy for the emission band is calculated from the known excited state vibronic energy (Ref. 19) minus the known vibrational energy in the ground state (Table III).

[b] The vibrational energy in the ground electronic state is not known. However, it was calculated using a set of vibrational constants given by Reisner *et al.* [J. Chem. Phys. **80**, 5968 (1984)].

[c] $f = 3.03\times10^{-6}(\Delta\tilde{\nu})|D|^2$ where $\Delta\tilde{\nu}$ is the vibronic transition frequency in cm^{-1} and D is the dipole length of the transition (Ref. 30). (−7) means 10^{-7}.

[d] The oscillator strengths for these combination bands could not be calculated as in footnote c.

[e] Probably much lower than the value for $4_1^2 6_1^1$ ($f = 5.8\times10^{-7}$).

cooled H_2CO molecules[24]: $A' = 8.918$, $B' = 1.105$, and $C' = 0.993\ cm^{-1}$. The rotational constants for $2^1 4^1 6^1$ determined from seven rotational transitions of $^qR_5(J'')$ observed with room temperature H_2CO molecules (see Tables II and III) are about 0.4% greater than the earlier determined values. Since the latter determination involves a measurement on the $K_a' = 5$ manifold with $J' = 6$–12, it should be more appropriate for the present work than the earlier determination on the $K_a' = 0$ and 1 manifolds with $J' = 0$–3 where Coriolis perturbation is negligible. In the present work, we were unable to observe an RELFEX spectrum of the $^qR_4(J'')$ subband or the $^qR_6(J'')$ subband, and therefore it has been difficult to improve the accuracy of the rotational constants listed in Table III. However, it is possible that some of the remaining unidentified peaks in the upper panel (b) of Fig. 3 are due to these subbands. A set of fluorescence emission spectra resulting from the excitation of these lines should provide the information required for an unambiguous identification of the upper states.

B. Patterns of H_2CO fluorescence emission

There are four C_{2v} vibrational symmetry species in H_2CO. Each species can give a characteristic pattern of fluorescence emission, because the H_2CO $\tilde{A}\,^1A_2$–$\tilde{X}\,^1A_1$ electronic transition is electric dipole forbidden but can be vibronically allowed. According to Strickler and Barnhart,[36] the oscillator strengths involving various antisymmetric vibrations are distributed as follows: ν_4 (66%), ν_5 (26%), ν_6 (6%), $\nu_4+\nu_5$ (0.5%), $\nu_4+\nu_6$ (0.5%), and an *A*-type magnetic dipole allowed transition (1%). This means that the *B*-type bands carry 66% of the oscillator strength and the *C*-type bands carry 32%. The results of the *ab initio* CI calculation of van Dijk *et al.*[31] are qualitatively consistent with the above analysis as shown in Tables VIII and IX. We expect, therefore, that in most cases *B*-type vibronic emission from a zero-order vibrational component of any upper

TABLE IX. Calculated oscillator strengths (f) for *B*- and *C*-type bands of the H_2CO $S_1 \leftarrow S_0$ transitions in the $E'_{vib} = 1800$–$2300\ cm^{-1}$ region.

Transition	Band type	Transition energy (cm^{-1})	Oscillator strength (f)
$4_0^1 6_0^2$	*B*	30 021[a]	3.69(− 8)[b]
4_0^5	*B*	30 138[a]	1.54(− 6)
$2_0^1 6_0^1$	*C*	30 252.21	1.82(− 6)
$2_0^1 4_0^3$	*B*	30 340.055	8.72(− 6)
$3_0^1 6_0^1$	*C*	30 362[a]	1.75(− 7)
$2_0^1 4_0^1 6_0^1$	*A*	30 395.0	...
$3_0^1 4_0^3$	*B*	30 450[a]	8.33(− 7)
$4_0^4 6_0^1$	*C*	30 521[a]	1.42(− 7)

[a] These transition energies represent calculated values as these bands have not been experimentally observed.
[b] (− 8) means 10^{-8}.

vibronic level should be favored over *C*-type emission and should clearly dominate over *A*-type emissions.

With the above simple guidelines, we can predict the following emission characteristics for *B*-type emission (within $\sim 3000\ cm^{-1}$ of the laser frequency) expected from *zero-order* vibrational components of an S_1 vibrational level: the $\mathbf{a}_1$ vibrational species give emissions to the ν_4'' and $(\nu_2'' + \nu_4'')$ levels; the $\mathbf{a}_2$ vibrational species give emissions to the ν_6'', ν_5'', and $(\nu_2'' + \nu_6'')$ levels; the $\mathbf{b}_1$ vibrational species give emissions to a set of $\mathbf{a}_1$ vibrational levels, ν_2'', $2\nu_4''$, and ν_1''; the $\mathbf{b}_2$ vibrational species give emissions to the $(\nu_4'' + \nu_6'')$ level. This prediction has already taken into account the fact that some vibrations, such as ν_1, ν_3, ν_5, and ν_6, are often optically inactive (i.e., $\Delta v_i = 0$) by Franck–Condon arguments. An example of the $\mathbf{a}_1$ zero-order vibrational component giving rise to the ν_4'' emission has been clearly shown in previous emission studies of the 5^1 and $1^1 4^1$ levels[16] which also provide an excellent example of the rotational intensity perturbations in emission (involving *B* and *C*-types) due to an **a**-axis Coriolis coupling. In the present work, we observe emissions mainly from the $\mathbf{a}_2$, $\mathbf{b}_1$, and $\mathbf{b}_2$ zero-order vibrational components in the excited eigenstates given in Fig. 1. We have limited our studies to emission terminating on the $\tilde{X}$ state levels below $E''_{vib} \simeq 3000\ cm^{-1}$, since the congestion in the emission spectrum becomes a serious problem above this energy.

C. $|2^1 4^1 6^1\rangle$ eigenstate emission

The $2_0^1 4_0^1 6_0^1 {}^qR_5(J'')$ rotational subband in Fig. 3(b) shows reasonable separations between individual rovibronic transition lines except in the case of the $J'' = 5$ and 7 lines which overlap significantly. Therefore, we have omitted these $J' = 6$ and 8 excitation transitions in preparing the S_1 levels for our emission study. The spectra from the $K'_a = 5$, $J' = 7$, 9, 10, and 11 levels showing the ν_6'' and $(\nu_4'' + \nu_6'')$ emission bands are given in Fig. 8, and the spectra from the $K'_a = 5$, $J' = 10$ and 11 levels to the $(\nu_2'' + \nu_6'')$ levels are shown in Fig. 7. The ν_6'' and $(\nu_2'' + \nu_6'')$ emission clearly characterizes the $2^1 4^1 6^1$ zero-order parent component, whereas the $(\nu_4'' + \nu_6'')$ emission gives evidence for the presence of the $\mathbf{b}_2$ zero-order mixed-in components (consisting of $2^1 6^1$, $3^1 6^1$, and $4^4 6^1$). The observed average of the frequency separation between the ${}^rQ$ and ${}^pQ$ lines of the ν_6'' emission band is $177 \pm 2\ cm^{-1}$ for the 5 J' levels listed in Table IV. This value together with the known ν_6'' rovibrational energies[25] unambiguously determines the K''_a quantum number to be 5. However, it is possible that the J values may be off by as much as 2.

Insignificant ν_2'' emission intensity is observed ($\leqslant 0.05$ compared to the intensity of the ν_6'' emission). Since the calculated oscillator strengths of $2_0^1 4_0^3$ and $2_0^1 4_0^1 6_1^1$ are similar ($\mathbf{f} = 7.1 \times 10^{-6}$ and 6.9×10^{-6}, respectively, in Table VIII), we can estimate from Eqs. (1) and (2) that the $2^1 4^1 6^1$ $K''_a = 5$ levels have $\leqslant 5\%$ character of $2^1 4^3$. The value of **f** $(2_0^1 4_1^1 6_0^1) = 1.3 \times 10^{-6}$ is ~ 5 times smaller than **f** $(2_0^1 4_0^1 6_1^1) = 6.9 \times 10^{-6}$ and the *C*-type emission to the ν_4'' levels should occur 120–150 cm^{-1} (14–18 Å) to the red of the *B*-type emission to the ν_6'' levels (we use the experimental rovibrational energies in the $K''_a = 4$ and 6 manifolds[25]). Therefore, the minor peaks appearing near 3430 Å could be due to weak *C*-type ${}^pP$ and ${}^pQ$ emission to the ν_4'' level. Again, it is obvious that *B*-type emission to the ν_4'' level from an $\mathbf{a}_1$ zero-order, mixed-in vibrational component cannot be substantiated, and we can justify neglecting the $\mathbf{a}_1$ mixed-in component.

The remaining problem here is the vibrational and rotational assignment of the emission lines observed in the 3560–3580 Å region. The observed transition frequencies for the $(\nu_4'' + \nu_6'')$ emission are listed in Table V, and the average value of the frequency differences between the ${}^rQ$ and ${}^pQ$ lines is $\sim 121 \pm 5\ cm^{-1}$ for $J' = 7$, 9, 10, and 11, whereas that between the ${}^rR$ and ${}^pP$ lines is $\sim 176 \pm 8\ cm^{-1}$. There is significantly more scatter for the $(\nu_4'' + \nu_6'')$ emission band than for the ν_6'' emission band in both line positions and intensity distributions. From the study of the 5^1 and $1^1 4^1$ emissions,[16] there are data for some rovibrational energy levels of $2\nu_4''$, $(\nu_4'' + \nu_6'')$, and $2\nu_6''$. The data for the 5^1, $J' = 6$, $K'_a = 6$ and $1^1 4^1$, $J' = 6$, $K'_a = 6$ emissions are particularly useful (see Tables II and III[16]). The frequency differences between the ${}^rR$ and ${}^pP$ emission lines of $(\nu_4'' + \nu_6'')$ are ~ 226 and $\sim 251\ cm^{-1}$, respectively.[16(b)]

These values of 226–251 cm^{-1} for the $K''_a = 5$ and 7 levels are in excess of the 50–75 cm^{-1} difference between ${}^rR$ and ${}^pP$ lines observed in our experiment. The magnitude of the difference would be reasonable if the final states were $K''_a = 3$ and 5 (instead of $K''_a = 5$ and 7) for the ${}^rR$ and ${}^pP$ lines, respectively, for the $(\nu_4'' + \nu_6'')$ emission as listed in Table V. Therefore, the $\mathbf{b}_2$ zero-order mixed-in emitting component must have $K'_a = 4$, as compared to $K'_a = 5$ of $2^1 4^1 6^1$ (parent component). This Coriolis resonance requires the Coriolis perturbing $\mathbf{b}_2$ level to have its vibrational origin at a higher energy, probably by 80–100 cm^{-1} (see Fig. 1), than the $2^1 4^1 6^1$ level. The $4^4 6^1$ level satisfies this requirement. However, there is yet an additional consideration to be examined.

We need to find a semiquantitative justification for how the $2_0^1 4_0^1 6_0^1$ transition acquires absorption intensity as well as how the $4^4 6^1$ component ($K'_a = 4$), rather than the $2^1 6^1$ component ($K'_a = 6$) or the $3^1 6^1$ ($K'_a = 5$ or 6) compo-

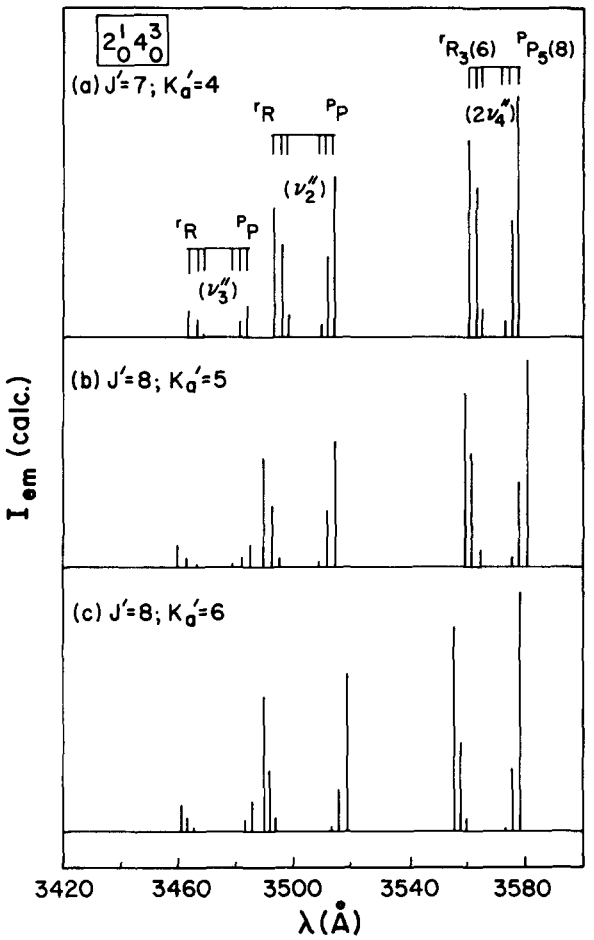

FIG. 9. The calculated rovibrational emission intensities from the three rovibrational levels of $2^1 4^3$ shown in Fig. 6 (see the text).

nent, provides the major part of the $(\nu_4'' + \nu_6'')$ emission intensity. In our preliminary report,[17] it was pointed out that two possibilities existed for the b_2 zero-order vibrational component of the emitting state: (i) $2^1 6^1$ $K_a' = 6$ component emitting to the $K_a'' = 5$ and 7 levels of $2\nu_4''$ as a *C*-type band, or (ii) $4^4 6^1$ $K_a' = 4$ component emitting to the $K_a'' = 3$ and 5 levels of $(\nu_4'' + \nu_6'')$. These zero-order states can interact with $2^1 4^1 6^1$ $K_a' = 5$ through **b**-axis Coriolis coupling.

The calculated emission oscillator strengths of $3_0^1 4_1^0 6_1^1$ and $4_1^4 6_1^1$ are 3.5×10^{-7} and $<5\times10^{-7}$, respectively, which are two orders of magnitude smaller than $\mathbf{f}(2_0^1 4_1^0 6_1^1) = 3.6\times10^{-5}$. The obvious choice for the major contributor to the $(\nu_4'' + \nu_6'')$ emission should then be $2^1 6^1$, and not $4^4 6^1$, on the basis of the rovibrational energy level structure discussed in the preceding paragraph. But, what if the calculated oscillator strengths are largely in error and the true zero-order oscillator strength of the $4_1^4 6_1^1$ transition is comparable to that of the $2_0^1 4_1^0 6_1^1$ transition? This certainly cannot be ruled out, and it could help rationalize the vibronic intensity-acquiring observed in the $2_0^1 4_0^1 6_0^1 {}^qR_5(J'')$ absorption band. As mentioned earlier, we have so far been unable to detect the "unseen" $4^4 6^1$ level by free-jet/fluorescence excitation spectroscopy, and this is rather disturbing.

The present assignment of the 3560–3580 Å band to the $(\nu_4'' + \nu_6'')$ $K_a'' = 3$ and 5 levels differs from the previous assignment to the $2\nu_4''$ $K_a'' = 5$ and 7 levels given in our preliminary report.[17] At the time, we did not have the information on the $2\nu_4''$, $(\nu_4'' + \nu_6'')$, and $2\nu_6''$ rovibrational energy levels which has been obtained from the fluorescence emission spectra of the 5^1 and $1^1 4^1$ rovibrational levels.[16(b)] From this recent information, we now know that the $2\nu_4''$ $K_a'' = 7$ levels are ~25 cm^{-1} above the $(\nu_4'' + \nu_6'')$ $K_a'' = 5$ levels, and some of the minor peaks slightly to the red of the main $(\nu_4'' + \nu_6'')$ emission lines in Fig. 7 could certainly be the $2\nu_4''$ emission features. Since $2\nu_4''$ and $(\nu_4'' + \nu_6'')$, perhaps also $2\nu_6''$,[16(b)] are perturbed by **a**-axis Coriolis interaction,[16(b),27] the excessive congestion observed in the 3560–3580 Å region is not surprising. We shall come back to this point for further discussion later.

In order to estimate the percentage which is of $|4^4 6^1\rangle$ character, we need to know zero-order **f** values that are reliable. However, if we accept an upper limit value of $\mathbf{f}(4_1^4 6_1^1) \simeq 7\times10^{-6}$, similar to $\mathbf{f}(2_0^1 4_0^1 6_1^1) = 6.9\times10^{-6}$ in Table VIII, and the observed emission intensities are estimated to be in a ratio of approximately 1:2 from Fig. 7, we can estimate that the $|2^1 4^1 6^1, J' = 7\text{–}11\rangle$ levels have $\sim60\%$ of $|2^1 4^1 6^1, J' = 7\text{–}11,\ K_a' = 5\rangle$ character, $\sim30\%$ of $|4^4 6^1, J' = 7\text{–}11, K_a' = 4\rangle$ character, and remaining 10% of $|2^1 4^3, J' = 7\text{–}11,\ K_a' = 6\rangle$ and $|2^1 6^1, J' = 7\text{–}11, K_a' = 6\rangle$ character.

D. $|2^1 4^3\rangle$ eigenstate emission

The $2_0^1 4_0^3 {}^rR_4(J'')$ and $^rR_5(J'')$ subbands in Figs. 2 and 3 show reasonable separation between individual rovibronic transition lines in most cases. The $2_0^1 4_0^3 {}^PP_5(J'')$, $^PP_6(J'')$, and $^PP_7(J'')$ subbands are somewhat less congested than the above *r*-form subbands (as shown elsewhere[30]); therefore, a cleaner preparation was obtained by pumping the *p*-form transitions, rather than the *r*-form transitions, for accessing the same S_1 rovibrational levels. A visual comparison is provided in Figs. 4 and 5 by the emission spectra taken by pumping two different transitions.

The emission spectra from the $2^1 4^3$ $K_a' = 4$ and 6 levels in Fig. 6 show the most intense feature to be ν_2'' emission, the weak feature to be ν_3'' emission, and the moderately intense feature to be $2\nu_4''$ emission. The calculated spectra using the **f** values of $2_0^1 3_1^0 4_0^3$, $2_1^1 4_0^3$, and $2_1^1 4_2^3$ and the Hönl–London rotational line strength formulae are shown in Fig. 9. A comparison of the two sets indicates that $\mathbf{f}(2_1^1 4_0^3)$ is too small and the $2_0^1 4_2^3$ lines show an anomalous rotational intensity distribution in which the *p*-form lines are suppressed by a Coriolis interaction in the $\tilde{X}$ state.[16,18] The strong appearance of ν_6'' emission from only the $2^1 4^3$ $K_a' = 5$ levels in Fig. 6 suggests that the otherwise weak $2_0^1 4_0^3 6_1^0$ transition acquires intensity through a Coriolis interaction, and this is very interesting and striking. Since the ν_6'' emission involves the $K_a'' = 3$ and 5 levels (via $2^1 4^3$ $K_a' = 5$ excitation) as assigned in Tables VI and VII, the unseen perturbing level must be $|2^1 4^1 6^1, J', K_a' = 4\rangle$ involved through **c**-axis Coriolis coupling. This is consistent with the Coriolis coupling schemes and energetics for resonances shown in Figs. 1 and 10, specifically the $2^1 4^3$ $(K_a' = 5)$: $2^1 4^1 6^1$ $(K_a' = 4)$ resonance.

The ratio of the emission band intensities, $I(\nu_6'')/I(\nu_2'')$, is a measure of *g*, the mixing coefficient for

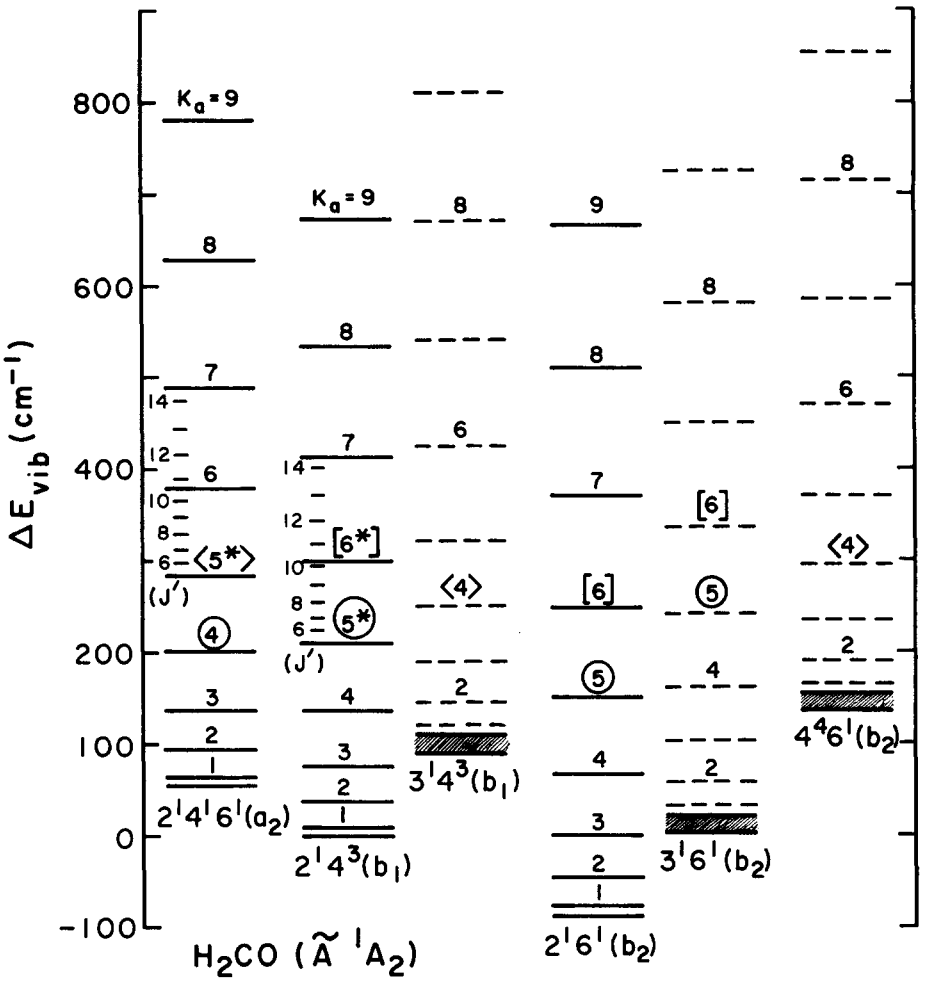

FIG. 10. A schematic rovibrational energy level diagram showing possible Coriolis resonance among various vibrational states. The K' manifold pumped is indicated by an asterisk. Each set of circles, brackets, and rectangular brackets enclosing K'_a quantum numbers indicates a set of K'_a values possible for resonance. The uncertainty in the vibrational origin is indicated by the hatched block.

$|2^1 4^1 6^1, J', K'_a = 4\rangle$ as shown in Eq. (3):

$$|2^1 4^1 6^1, J'\rangle = d\,|2^1 4^3, J, K'_a = 5\rangle - i\sigma_{\zeta k} g |2^1 4^1 6^1, J', K'_a = 4\rangle.^{16,18} \quad (3)$$

It can be ascertained from the relative intensities in Fig. 4 for various values of J'. It increases almost linearly from a value of ~ 0.4 at $J' = 5$ to a value of ~ 0.9 at $J' = 11$. The values of the oscillator strengths are $f(2_0^1 4_0^1 6_1^1) = 6.9 \times 10^{-6}$ and $f(2_1^1 4_0^3) = 7.1 \times 10^{-6}$. Therefore, the ratio of mixing coefficients (g/d) increases from a value of ~ 0.4 at $J' = 5$ to ~ 0.9 at $J' = 11$ for the $2^1 4^3$ $K'_a = 5$ manifold, and it is less than 0.1 for the $2^1 4^3$ $K'_a = 4$ and 6 manifolds.

The intensity suppression observed for the p-form subband of the $2\nu_4''$ emission can be interpreted as the result of interference between the B-type emission (connecting $|2^1 4^3\rangle$ with $|4_2\rangle$) and the C-type emission (connecting $|2^1 4^3\rangle$ with $|4_1 6_1\rangle$) as found for the 5_0^1 and $1_0^1 4_0^1$ bands studied earlier.[16,18] As mentioned in Sec. IV C, the 4_2, $4_1 6_1$, and 6_2 levels exist as a Coriolis triad linked by a-axis couplings. To simplify matters, let us ignore the role $|6_2\rangle$ may play and consider only the a-axis Coriolis interaction between $|4_2\rangle$ and $|4_1 6_1\rangle$. The calculated values of the oscillator strengths listed in Table VIII which are of interest here are $f(2_0^1 4_2^3) = 1.3 \times 10^{-5}$ and $f(2_0^1 4_1^3 6_1^0) = 1.7 \times 10^{-6}$. According to theory,[16,18] a complete intensity suppression, i.e., destructive interference, of the p-form (or r-form) intensity by Coriolis interactions occurs, if the magnitude of the transition moments are equal and furthermore the mixing coefficients are equal for the *zero-order* transitions $2_0^1 4_2^3$ and $2_0^1 4_1^3 6_1^0$. Since complete intensity suppression of the p-form subband is observed, one or both of the above two calculated values cannot be correct, and we must conclude that $f(2_0^1 4_2^3) = f(2_0^1 4_1^3 6_1^0)$. We also expect, therefore, that at the low values of K''_a where the Coriolis interaction decreases, and hence $|4_2\rangle$ mixes less with $|4_1 6_1\rangle$, we should observe the trend for restoring the normal rotational line intensity profile. This is not yet apparent even for the $2^1 4^3$ $K'_a = 4$ level shown in Fig. 6, indicative of the persistent mixing of $|4_2\rangle$ and $|4_1 6_1\rangle$. Of course, the consideration of $|6_2\rangle$ should introduce more complication to the simplified situation depicted so far.

There is one minor feature in Fig. 6 worth mentioning. There are two weak but distinct peaks labeled as $\nu_4''^q P$ and $\nu_6''^q P$ for the $J' = 8$, $K'_a = 6$ level [Fig. 6(c)]. We believe that these lines probably acquire intensity through Coriolis interaction between an a_1 mixed-in component and the $2^1 4^3$ parent and between an a_2 mixed-in component and the $2^1 4^3$ parent as illustrated by the previous examples.[16,35] For the $J' = 7, K'_a = 4$ level [Fig. 6(a)], two additional weak peaks appear in this region, but we will not attempt to consider the origin of these peaks.

TABLE X. $2^1 4^3$ $K'_a = 5$ energy and intensity perturbations brought about by interaction with $2^1 4^1 6^1$ $K'_a = 4$ ($\Delta J = 0$; $\Delta K_a = -1$).

J	$[J(J+1) - K_a(K_a-1)]$	$\Delta E_{\text{obs-calc}}$ (cm^{-1})[a]	$\xi_{st}^{(c)}$ (cm^{-1})[b]	$\frac{I_{em}(\nu''_6)}{I_{em}(\nu''_2)}$
5	10	−0.01	...	0.43
6	22	−0.11	0.15_8	0.45
7	36	−0.30	0.20_4	0.61
8	52	−0.35	0.18_3	0.70
9	70	−0.43	0.17_5	0.82
10	90	−0.51	0.16_8	...
11	112	−0.61	0.16_5	0.90
12	136	−0.69	0.15_6	...
13	162	−0.76	0.15_3	...
		Av.	$0.15_0 \pm 0.06$[c]	

[a] We used $\Delta E_{v,r}$ ($2^1 4^1 6^1$–$2^1 4^3$) $\simeq 1.25$ cm^{-1} for these levels which were calculated from the rotational constants listed in Table III.

[b] $|s\rangle = |2^1 4^3\rangle$, $|t\rangle = |2^1 4^1 6^1\rangle$ and $\xi_{st}^{(c)}$ is defined by $\langle v_t, J, k | H_{\text{Coriolis}} | v_s, J, k \pm 1\rangle = +(1/2)\xi_{st}^{(c)} F(J,k)$ where $F(J,k) = [J(J+1) - k(k \pm 1)]^{1/2}$ (Ref. 25).

[c] Represents one standard deviation.

E. Energy perturbation in the $2^1 4^3$ $K'_a = 5$ stack

In the preceding section, c-axis Coriolis perturbation between rotational levels of $2^1 4^3$ $K'_a = 5$ and $2^1 4^1 6^1$ $K'_a = 4$ has been examined by fluorescence emission spectroscopy. Now the same interaction can be analyzed in terms of energy level shifts as done previously for the $2^1 4^3$ levels by Sethuraman *et al.*,[20] however using the new sets of rotational constants for $2^1 4^3$ and $2^1 4^1 6^1$.

Using the rotational constants given in Table III, the energies of these rotational levels were computed by an asymmetric rotor program. Since the rotational constants were derived from the data for the $2^1 4^3$ $K'_a = 0-4$, $J' \leqslant 12$ (Ref. 21) and $2^1 4^1 6^1$ $K'_a = 0$ and 5, $J' \leqslant 12$ (Ref. 24 and Table III), the calculated level energies are subject to some degree of Coriolis perturbation in these manifolds. An approximate value of detuning from the $K'_a = 5$ vs 4 resonance can be obtained. The values of $\Delta E_{v,r} = E_{v,r}(2^1 4^1 6^1) - E_{v,r}(2^1 4^3)$ have the following ranges of variation; ~ 11 cm^{-1} for $J' = 4 \sim 13$ in the $2^1 4^3$ $K'_a = 4$ stack; ~ 1.25 cm^{-1} for $J' = 5 \sim 13$ in the $2^1 4^3$ $K'_a = 5$ stack; $-10(-11)$ cm^{-1} for $J' = 6$–13 in the $2^1 4^3$ $K'_a = 6$ stack. The near resonance at $K'_a = 5$ ($2^1 4^3$) and $K'_a = 4$ ($2^1 4^1 6^1$) is verified. From these data, it is tempting to calculate the energy level shifts and the mixing coefficients using perturbation theory, although we do not have accurate data on the perturbed energies. The results are presented for $2^1 4^3$ ($K'_a = 5$) in Table X. We calculate the value of the c-axis Coriolis coupling constant $\xi_{st}^{(c)}$ for the $2^1 4^3(s)$ and $2^1 4^1 6^1(t)$ interaction to be ~ 0.15 cm^{-1}; its accuracy should be poor, because the preperturbed energy gap of $\Delta E_{v,r}(2^1 4^1 6^1$–$2^1 4^3) = 1.25$ cm^{-1} for the $2^1 4^3, J' = 5$–$13, K'_a = 5$ and $2^1 4^1 6^1, J' = 5$–$13, K'_a = 4$ levels is not known accurately. An error of a factor of 2 would not be surprising, since many of the $2^1 4^3$ levels are perturbed extensively by various mechanisms.[20,21] However, this value is several times smaller than those reported for b and c-axis Coriolis coupling constants for S_0 vibrational levels.

F. Vibrational mixing

With excess vibrational energy in the $\tilde{A}$ state of only ~ 2000 cm^{-1}, excitations of the in-plane and out-of-plane skeletal bending vibrational modes and the C–O stretching mode are possible, but excitation of the C–H stretching modes are not possible energetically. In the present study, we have been able to observe vibrational mixing on the S_1 manifold involving mainly two vibrational modes, $\nu'_4(b_1)$ and $\nu'_6(b_2)$ in the $E'_{\text{vib}} = 2000$–2300 cm^{-1} region, whereas vibrational mixing involving mainly the C–H stretching (ν'_1 and ν'_5) modes and the out-of-plane bending (ν'_4) mode was examined previously in the $E'_{\text{vib}} \simeq 3000$ cm^{-1} region.[16] In the former, we observe two separate cases of two-state mixing, $2^1 4^3$ ($K'_a = 5$) with $2^1 4^1 6^1$ ($K'_a = 4$) and $2^1 4^1 6^1$ ($K'_a = 5$) with $4^4 6^1$ ($K'_a = 4$), whereas two separate cases of three-state mixing, 5^1 (K'_a) with $1^1 4^1$ (K'_a) and $\mathbf{a}_1$ (such as $2^2 4^2, K'_a + 1$), and $1^1 4^1$ (K'_a) with 5^1 (K'_a) and $\mathbf{a}_1$ (such as $2^2 4^2, K'_a + 1$) are seen in the latter. From these cases, the means of gaining quantitative information about the degree of rotation-induced vibrational mixing in S_1 H_2CO are well demonstrated, and it is clear that the present fluorescence emission probe can be applied to studies of other polyatomic molecules. One noteworthy result of these studies is that, although K_a is truly not a good quantum number, we were able to keep track of it in the emission spectrum, since we have not yet encountered an example of $|\Delta K_a| \geqslant 2$. So far, the extent of the vibrational mixing is restricted to $|\Delta K_a| = 0$ and 1, because the density of vibrational states is sparse ($\rho \simeq 0.1$ per cm^{-1}) and the rotational quantum number is relatively low ($J \leqslant 15$). However, one could encounter a more interesting situation of $|\Delta K_a| \gg 2$ and multistate mixing which approaches a close approximation of IVR.[8,9(b),14] An extension of the present study to high regions of E'_{vib} where multistate mixing should manifest itself is currently under investigation in our laboratory.

ACKNOWLEDGMENTS

The kind cooperation of Dr. D. A. Ramsay and Mr. W. S. Neil of the Herzberg Institute of Astrophysics, National Research Council, Ottawa, Canada, in obtaining the FTUV spectra is gratefully acknowledged.

[1] K. F. Freed and A. Nitzan, J. Chem. Phys. **73**, 4765 (1980).
[2] R. A. Marcus, Faraday Discuss. Chem . Soc. **75**, 103 (1983).
[3] K. von Puttkamer, H.-R. Dübal, and M. Quack, Faraday Discuss. Chem. Soc. **75**, 197 (1983).
[4] E. J. Heller, Faraday Discuss. Chem. Soc. **75**, 141 (1983).
[5] (a) S. Mukamel, J. Phys. Chem. **89**, 1077 (1985); (b) J. Chem. Phys. **82**, 2867 (1985).
[6] (a) C. S. Parmenter, J. Phys. Chem. **86**, 1735 (1982); (b) Faraday Discuss. Chem. Soc. **75**, 7 (1983).
[7] (a) R. E. Smalley, J. Phys. Chem. **86**, 3504 (1982); (b) Annu. Rev. Phys. Chem. **34**, 129 (1983).
[8] (a) G. Stewart, R. Ruoff, T. Kulp, and J. D. McDonald, J. Chem. Phys. **80**, 5353 (1984); (b) T. Kulp, R. Ruoff, G. Stewart, and J. D. McDonald, *ibid.* **80**, 5359 (1984); (c) J. D. McDonald, *ibid.* **82**, 2175 (1985).
[9] (a) H.-L. Dai, C. L. Korpa, J. L. Kinsey, and R. W. Field, J. Chem. Phys. **82**, 1688 (1985); (b) H.-L. Dai, R. W. Field, and J. L. Kinsey, *ibid.* **82**, 2163 (1985).
[10] (a) E. Riedle, H. J. Neusser, and E. W. Schlag, J. Phys. Chem. **86**, 4847 (1982); (b) E. Riedle, and H. J. Neusser, J. Chem. Phys. **80**, 4686 (1984).
[11] (a) H. Saigusa, B. E. Forch, and E. C. Lim, J. Chem. Phys. **78**, 2795

(1983); (b) K. T. Chen, B. E. Forch, and E. C. Lim, Chem. Phys. Lett. **99**, 98 (1983).
[12](a) P. M. Felker and A. H. Zewail, Chem. Phys. Lett. **102**, 113 (1983); (b) **108**, 303 (1984).
[13]J. G. Haub and B. J. Orr, Chem. Phys. Lett. **107**, 162 (1984).
[14](a) C. L. Chen, B. Maessen, and M. Wolfsberg, J. Chem. Phys. **83**, 1795 (1985); (b) B. Maessen and M. Wolfsberg, J. Phys. Chem. **89**, 3876 (1985).
[15](a) A. Hodgson, J. P. Simons, M. N. R. Ashfold, J. M. Bayley, and R. N. Dixon, Mol. Phys. **54**, 351 (1985); (b) M. N. R. Ashfold, J. M. Bailey, and R. N. Dixon, Can. J. Phys. **62**, 1806 (1984).
[16](a) N. L. Garland and E. K. C. Lee, Faraday Discuss. Chem. Soc. **75**, 377 (1983); (b) J. Chem. Phys. **84**, 28 (1986).
[17]E. C. Apel and E. K. C. Lee, J. Phys. Chem. **88**, 1283 (1984).
[18]R. Nanes and E. K. C. Lee, J. Chem. Phys. **84**, 5290 (1986).
[19]D. J. Clouthier and D. A. Ramsay, Annu. Rev. Phys. Chem. **34**, 31 (1983).
[20](a) V. Sethuraman, V. A. Job, and K. K. Innes, J. Mol. Spectrosc. **33**, 189 (1970); (b) V. A. Job, V. Sethuraman, and K. K. Innes, *ibid.* **30**, 365 (1969).
[21]C. M. L. Kerr, D. C. Moule, and D. A. Ramsay, Can. J. Phys. **61**, 6 (1983).
[22](a) D. L. Holtermann, E. K. C. Lee, and R. Nanes, J. Chem. Phys. **77**, 5327 (1982); (b) D. L. Holtermann, Ph.D. thesis, University of California, Irvine, 1981.
[23]S. Gerstenkorn and P. Luc, *Atlas of the Absorption Spectrum of I_2 (14,800–20,000 cm^{-1})* (CNRS, Paris, 1978).
[24]E. C. Apel and E. K. C. Lee, J. Phys. Chem. **89**, 1391 (1985).
[25]M. Allegrini, J. W. C. Johns, and A. R. W. McKellar, J. Mol. Spectrosc. **67**, 476 (1977).
[26]C. Bréchignac, J. W. C. Johns, A. R. W. McKellar, and M. Wong, J. Mol. Spectrosc. **96**, 353 (1982).
[27]J. L. Hardwick and S. M. Till, J. Chem. Phys. **70**, 2340 (1979).
[28]D. E. Reisner, R. W. Field, J. L. Kinsey, and H.-L. Dai, J. Chem. Phys. **80**, 5968 (1984).
[29]L. R. Brown, R. H. Hunt, and A. S. Pine, J. Mol. Spectrosc. **75**, 406 (1979).
[30]E. C. Apel, E. K. C. Lee, and D. A. Ramsay (in preparation).
[31]J. M. F. van Dijk, M. J. H. Kemper, J. H. M. Kerp, and H. M. Buck, J. Chem. Phys. **69**, 2453 (1978).
[32]P. W. Fairchild, K. Shibuya, and E. K. C. Lee, J. Chem. Phys. **75**, 3407 (1981).
[33]B. J. Orr, J. G. Haub, G. F. Nutt, J. L. Steward, and O. Vozzo, Chem. Phys. Lett. **78**, 621 (1981).
[34]E. C. Apel and E. K. C. Lee, J. Chem. Phys. **84**, 1039 (1986).
[35]C. M. L. Kerr and D. A. Ramsay, J. Mol. Spectrosc. **87**, 575 (1981).
[36]S. J. Strickler and R. J. Barnhart, J. Phys. Chem. **86**, 448 (1982). The intensity of the $\nu_4' \nu_6'$ combination band in the H_2CO $\tilde{A} \leftarrow \tilde{X}$ transition is 0.5% of the total electronic oscillator strength as compared to that of the ν_4' band which carries 66% of the total oscillator strength.
[37](a) I. M. Mills, Pure Appl. Chem. **11**, 325 (1965); (b) I. M. Mills, W. L. Smith, and J. L. Duncan, J. Mol. Spectrosc. **16**, 349 (1965).
[38]T. Nakagawa, H. Kashiwagi, H. Kurihara, and Y. Morino, J. Mol. Spectrosc. **31**, 436 (1969).